

# Fitting Effective Field Theory to $\Xi$ - $\Xi$ lattice QCD results

Author: Daniel Ayyash Sala

Advisor: Joan Soto

*Facultat de Física, Universitat de Barcelona, Diagonal 645, 08028 Barcelona, Spain\**

**Abstract:** we fit lattice QCD results of baryon-baryon potentials in the strangeness  $S=-4$  sector using the Effective Field Theory (EFT) and show how good this fit is. Next, we estimate some physical parameters associated to this interaction. These parameters include scattering length and the  $\Xi$  axial coupling constant ( $g_A$ ). Finally, we compare our results to One Boson Exchange models.

## I. INTRODUCTION

Quantum chromodynamics is the fundamental theory which explains the strong interaction. Despite its success, QCD has not been able to explain successfully processes that involve baryons and mesons. The reason why is that at low energies the couplings of quarks and gluons become so large that is not possible to treat the problem in a perturbative way. But, at high energies (due to asymptotic freedom) it is possible.

The EFT approach consist of a low energy realization of QCD at hadronic level. The EFT includes the degrees of freedom relevant at low energy, while preserving QCD symmetries. The terms obtained in this way can be sorted out by the development parameter  $(Q/\Lambda)^v$ , leading to a contribution hierarchy (Q and  $\Lambda$  corresponding to low and high energy scale).

The effective field theory that describes the physics of hadronic processes is known as chiral perturbation theory (ChPT).

Weinberg suggested to calculate nucleon-nucleon potential in two steps: the first one was calculating order by order the nucleon-nucleon (NN) potential using ChPT and then introducing the potentials thus obtained in a Lippmann-Schwinger (or Schrödinger) equation.

We are allowed to use EFT to describe  $\Xi$ - $\Xi$  interaction, because of this theory only takes into account the symmetries:  $\Xi$  and N both have the same Spin and Isospin. That fact leads to the same leading order (LO) and next to leading order (NLO) potentials obtained in NN, but with different parameters, such as  $g_A$ , the axial coupling constant.

In this project we will confine ourselves to use the  $\Xi$ - $\Xi$  potentials thus obtained at leading order and at next to leading order. We also will only consider the  $^1S_0$  and  $^3S_1$  channels, which are the most relevant ones at low energy.

## II. POTENTIALS AT LO AND NLO

In the ChPT the potentials are made up of two type of terms: contact terms and pion exchange terms. Figure 1 shows the associated diagrams at LO and NLO. In [5] we can find the associated Lagrangians in both orders, but we are not going to write them owing to space needs.

- At LO,  $(Q/\Lambda)^0$ , the potential is made up of One Pion Exchange (OPE) potential (coming from 1 one-pion exchange diagram) and  $\delta^3(\mathbf{r})$  (coming from the contact Lagrangian at LO).
- A NLO,  $(Q/\Lambda)^2$ , we have to add the Two Pion Exchange (TPE) potential (coming from 5 two-pion

exchange diagrams) and a  $\vec{\nabla}^2\delta^3(\mathbf{r})$  (coming from the contact Lagrangian at NLO).

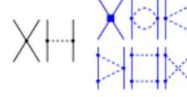


Figure 1: LO (left) and NLO (right) diagrams. Solid lines represent nucleons and dashed lines pions.

### A. Contact terms

Owing to the fact that EFT is based on a Lagrangian with local meson-nucleon coupling, multi-meson exchange processes lead to a potential that is highly singular at short distances. To renormalize these short-distances (UV) divergences one has to introduce counterterms in the Lagrangian and hence any dependence on physical scales much higher than the ones of the problem at hand can be encoded in few low energy constants [1]. These take the form of the following contact terms of the Lagrangian in the momentum expansion:  $(\bar{\Psi}\Psi)^2$  at LO and  $(\bar{\Psi}\Psi)(\bar{\Psi}\vec{\nabla}^2\Psi)$  at NLO, where  $\Psi$  stands for the baryon field.

From [5], we present the contact NN potentials at LO and at NLO (momentum space). We will present only the projections of these potentials corresponding to  $^1S_0$  and  $^3S_1$  channels.

- At LO:  $\begin{cases} V_{1S_0} = C_S - 3C_T \equiv a_1 \\ V_{3S_1} = C_S + C_T \equiv a_2 \end{cases}$
- At NLO:  $\begin{cases} V_{1S_0} = b_1 \cdot \mathbf{k}^2 \\ V_{3S_1} = b_2 \cdot \mathbf{k}^2 \end{cases}$

Where  $a_1$ ,  $a_2$ ,  $b_1$ ,  $b_2$  are fitting constants and  $\mathbf{k}$  is the momentum transfer.

We apply Fourier Transformation in order to obtain them in the r-space:

$$V_{LO}(\mathbf{r}) = \frac{1}{(2\pi)^3} \int_{\mathbf{R}^3} a_i e^{i\mathbf{k}\cdot\mathbf{r}} d^3\mathbf{k} = a_i \delta^3(\mathbf{r}), \quad i = 1, 2. \quad (1)$$

$$V_{NLO}(\mathbf{r}) = \frac{1}{(2\pi)^3} \int_{\mathbf{R}^3} b_i \mathbf{k}^2 e^{i\mathbf{k}\cdot\mathbf{r}} d^3\mathbf{k} = b_i \vec{\nabla}^2 \delta^3(\mathbf{r}), \quad i = 1, 2. \quad (2)$$

In order to eventually compare with numerical data,  $\delta^3(\mathbf{r})$  and  $\vec{\nabla}^2\delta^3(\mathbf{r})$  will be regulated as follows:

$$\delta^3(\mathbf{r}) = \left(\frac{\Lambda}{\sqrt{\pi}}\right)^3 \cdot e^{-\Lambda^2 \cdot r^2}.$$

$$\vec{\nabla}^2\delta^3(\mathbf{r}) = \frac{1}{r} \frac{\partial}{\partial r} \left( r \frac{\partial}{\partial r} \right) \delta^3(\mathbf{r}) = (-4\Lambda^2 + 4\Lambda^4 r^2) \delta^3(\mathbf{r}).$$

\* Electronic address: dayyassa7@alumnes.ub.edu

Where  $\Lambda$  is the cut-off. This cut-off has to absorb any dependence on physical scales much higher than the ones of the problem at hand (Ref. [1]).

### B. One Pion Exchange

We take de LO NN-potential (k-space) given in ref [1], and using the Fourier Transformation, we obtain the following expression in r-space:

$$V(\mathbf{r}) = \frac{1}{48\pi} \left( \frac{g_A}{f_\pi} \right)^2 m_\pi^2 \boldsymbol{\tau}_1 \boldsymbol{\tau}_2 \left\{ \left[ S_{12} \left( 1 + \frac{3}{m_\pi r} + \frac{3}{(m_\pi r)^2} \right) + \boldsymbol{\sigma}_1 \boldsymbol{\sigma}_2 \right] \frac{e^{-m_\pi r}}{r} - \frac{4\pi}{3} \boldsymbol{\sigma}_1 \boldsymbol{\sigma}_2 \delta^3(\mathbf{r}) \right\} \quad (3)$$

Where  $g_A$  is the nucleon axial-vector strength,  $f_\pi = 93 \text{ MeV}$  is the pion decay constant,  $m_\pi = 138 \text{ MeV}$ ,  $\boldsymbol{\sigma}_1, \boldsymbol{\sigma}_2$  and  $\boldsymbol{\tau}_1, \boldsymbol{\tau}_2$  are the spin and isospin operators of each nucleon.  $S_{12} = \hat{\mathbf{r}} \cdot \boldsymbol{\sigma}_1 \hat{\mathbf{r}} \cdot \boldsymbol{\sigma}_2 - \boldsymbol{\sigma}_1 \boldsymbol{\sigma}_2$  is only non-zero when the angular momentum of the initial and final states differs by  $\Delta L = 2$  [4]. So, for initial and final state S-waves, it does not contribute. This leads to a simplified expression in our both channels (ignoring  $\delta$  term):

$$V(\mathbf{r}) = \frac{1}{48\pi} \left( \frac{g_A}{f_\pi} \right)^2 m_\pi^2 \tau_1 \tau_2 \sigma_1 \sigma_2 \frac{e^{-m_\pi r}}{r} \quad (4)$$

Notice that LO potential is written as a two factors sum. The first one is the OPE potential and the second is the contact term at LO.

Now, let's see spin and isospin projections for each channel:

$$\begin{aligned} \langle \boldsymbol{\sigma}_1 \boldsymbol{\sigma}_2 \rangle &= \begin{cases} -3, & S = 0, I = 1 \rightarrow \text{spin - singlet} \\ 1, & S = 1, I = 0 \rightarrow \text{spin - triplet} \end{cases} \\ \langle \boldsymbol{\tau}_1 \boldsymbol{\tau}_2 \rangle &= \begin{cases} 1, & S = 0, I = 1 \rightarrow \text{spin - singlet} \\ -3, & S = 1, I = 0 \rightarrow \text{spin - triplet} \end{cases} \end{aligned}$$

According to this projections, we have in both channels that  $\langle \boldsymbol{\tau}_1 \boldsymbol{\tau}_2 \boldsymbol{\sigma}_1 \boldsymbol{\sigma}_2 \rangle = -3$ . So, the OPE potential has exactly the same shape:

$$V_{1S_0}^{OPE}(\mathbf{r}) = V_{3S_1}^{OPE}(\mathbf{r}) = -\frac{1}{16\pi} \left( \frac{g_A}{f_\pi} \right)^2 m_\pi^2 \frac{e^{-m_\pi r}}{r} \quad (5)$$

### C. Two Pion Exchange

At NLO, TPE potential expression in r-space (neglecting contributions suppressed by the  $\Xi$  mass) given in Ref. [3] and Ref. [6] are:

$$V_{1S_0}^{TPE} = \frac{1}{8\pi^3} \frac{m_\pi}{(2f_\pi)^4} \frac{1}{r^4} \{ x(1 + 10g_A^2 - g_A^4(59 + 4x^2)) \cdot K_0(2x) + (1 + 10g_A^2 - 59g_A^4 + (4g_A^2 - 36g_A^4)x^2) \cdot K_1(2x) \} \quad (6)$$

$$V_{3S_1}^{TPE} = \frac{1}{8\pi^3} \frac{m_\pi}{(2f_\pi)^4} \frac{1}{r^4} \{ x((81 + 12x^2)g_A^4 - 3 - 30g_A^2) \cdot K_0(2x) + ((81 + 44x^2)g_A^4 - 3 - (30 + 12x^2)g_A^2) \cdot K_1(2x) \} \quad (7)$$

Where  $x = m_\pi \cdot r$  and  $K_n(2x)$  are the modified Bessel functions.

## III. LATTICE QCD RESULTS ON $\Xi$ - $\Xi$ INTERACTION

In Ref. [7] N. Ishii et al. present baryon-baryon potentials in  $S = -3, -4$  sectors. They are constructed using HAL QCD method based on the Nambu-Bethe-Salpeter (NBS) wave functions generated by lattice QCD. Pion mass is stated at  $m_\pi = 146 \text{ MeV}$ . It includes the  $\Xi\Xi$  potential plot in  $^1S_0$  with  $I = 1$ , and in  $^3S_1$  with  $I = 0$  respectively. We have extracted these data from their FIG. 1, taking potential values from  $0.4 \text{ fm}$  to  $2.0 \text{ fm}$ , using a  $0.1 \text{ fm}$  step. We have also included an error bar for each potential value:

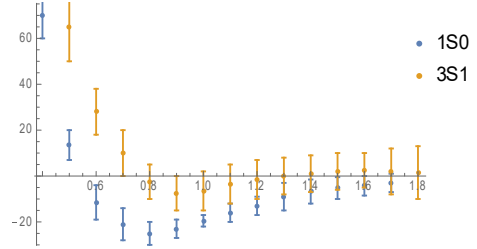


Figure 2:  $\Xi\Xi$  potential plot in  $^1S_0$  with  $I = 1$ , and in  $^3S_1$  with  $I = 0$ .

As we can see, error bars are very significant. So we have to be aware that this fact will condition our fits.

## IV. FITTING DATA WITH EFT

In this section, we will fit the potentials at LO and at NLO (at  $^1S_0$  and  $^3S_1$  channels) obtained in section II to the data extracted from [7], which is shown in Figure 2.

*Initial considerations:*

- NN axial coupling constant value is well-known. But, taking into consideration that this constant is not constrained by the symmetries, we can expect a different value of the constant in the  $\Xi\Xi$  system. So, we will treat  $g_A$  as a fitting parameter.
- In order to fit the potentials, we will use *Wolfram Mathematica* function *NonLinearModelFit[]*. That function gives us the fitted function together with the estimated parameters and their confidence intervals.
- Estimated parameters will be presented in the confidence interval provided by *Wolfram Mathematica* function *NonLinearModelFit[]*.
- We will include two additional fitting parameters ( $V_0, V_0'$ ). They correspond to the potential value at infinity and are introduced in order to readdress any data shift.
- The fit will be done simultaneously for the both channels ( $1S_0, 3S_1$ ) so that the cut-off ( $\Lambda$ ) and de  $g_A$  will be a common parameter while the other parameters ( $V_0$  or the parameter that multiplies  $\delta$ 's functions) will be different for each channel.

- In order to estimate the goodness of this fit, we will use  $\chi^2$  test:

$$\chi^2 = \frac{1}{N - d - 1} \sum_{i=1}^n \frac{(V_i - f(r_i))^2}{(err_i)^2} \quad (8)$$

Where  $V_i$  is the potential value at  $r_i$ ,  $err_i$  its associated error,  $f(\cdot)$  is the fitted function.  $N$  is the number of potentials values we are fitting and  $d$  is the degrees of freedom (number of fitting parameters).

As much closer  $\chi^2$  gets to 1 much better will be the fit. Fits with  $\chi^2 < 1$  usually reflect large errors in the data and hence a certain freedom to describe data with different functions.

### A. Leading Order

- As we have seen, at LO, potentials have the following form:

$$V_{1S_0}^{LO} = V_0 + a_1 \cdot \left(\frac{\Lambda}{\sqrt{\pi}}\right)^3 \cdot e^{-\Lambda^2 \cdot r^2} + V_{1S_0}^{OPE}(\mathbf{r}) \quad (9)$$

$$V_{3S_1}^{LO} = V'_0 + a_2 \cdot \left(\frac{\Lambda}{\sqrt{\pi}}\right)^3 \cdot e^{-\Lambda^2 \cdot r^2} + V_{3S_1}^{OPE}(\mathbf{r}) \quad (10)$$

Where  $a_1$ ,  $a_2$ ,  $\Lambda$  are fitting parameters.

- LO fitting outcome is presented below:

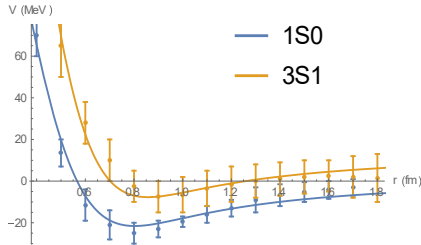


Figure 3: Channels 1s0 3s1. Fitting at LO.

	<i>Expected value</i>	<i>Confidence interval</i>
$\Lambda$	521 MeV	[470 MeV, 567 MeV]
$a_1$	$\frac{1}{(247 \text{ MeV})^2}$	$\left[\frac{1}{(270 \text{ MeV})^2}, \frac{1}{(230 \text{ MeV})^2}\right]$
$a_2$	$\frac{1}{(241 \text{ MeV})^2}$	$\left[\frac{1}{(230 \text{ MeV})^2}, \frac{1}{(180 \text{ MeV})^2}\right]$
$g_A$	1.95	[1.4, 2.3]

Table 1: Estimated parameters (LO).

- Fit goodness:  $\begin{cases} \chi^2_{1S_0} = 0.58 \\ \chi^2_{3S_1} = 0.20 \end{cases}$

### B. Next to Leading Order

At NLO we came up with the linear combination of  $\delta^3(\mathbf{r})$  and  $\vec{\nabla}^2 \delta^3(\mathbf{r})$ , which is written as follows:  $(a_i - 4b_i \Lambda^2 +$

$4b_i \Lambda^4 r^2) \left(\frac{\Lambda}{\sqrt{\pi}}\right)^3 e^{-\Lambda^2 \cdot r^2}$ , where parameters  $a_i$  and  $b_i$  ( $i = 1, 2$ ) are defined in section II.

- As we have seen, at NLO, the potentials have the following form:

$$V_{1S_0}^{NLO} = V_0 + (a_1 - 4b_1 \Lambda^2 + 4b_1 \Lambda^4 r^2) \left(\frac{\Lambda}{\sqrt{\pi}}\right)^3 e^{-\Lambda^2 \cdot r^2} + V_{1S_0}^{OPE}(\mathbf{r}) + V_{1S_0}^{TPE}(\mathbf{r}) \quad (11)$$

$$V_{3S_1}^{NLO} = V'_0 + (a_2 - 4b_2 \Lambda^2 + 4b_2 \Lambda^4 r^2) \left(\frac{\Lambda}{\sqrt{\pi}}\right)^3 e^{-\Lambda^2 \cdot r^2} + V_{3S_1}^{OPE}(\mathbf{r}) + V_{3S_1}^{TPE}(\mathbf{r}) \quad (12)$$

- NLO fitting outcome is presented below:

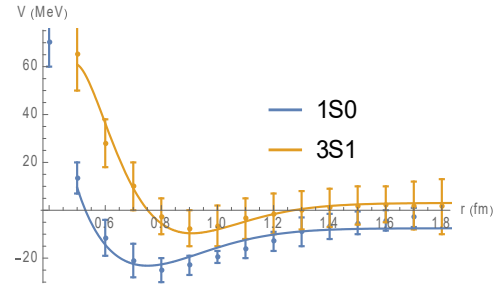


Figure 5: Channels 1s0 3s1. Fitting at NLO.

	<i>Expected value</i>	<i>Confidence interval</i>
$\Lambda$	398 MeV	[371 MeV, 424 MeV]
$a_1$	$\frac{1}{(210 \text{ MeV})^2}$	$\left[\frac{1}{(232 \text{ MeV})^2}, \frac{1}{(185 \text{ MeV})^2}\right]$
$a_2$	$\frac{1}{(167 \text{ MeV})^2}$	$\left[\frac{1}{(191 \text{ MeV})^2}, \frac{1}{(145 \text{ MeV})^2}\right]$
$b_1$	$-\frac{1}{(441 \text{ MeV})^4}$	$\left[-\frac{1}{(407 \text{ MeV})^4}, -\frac{1}{(500 \text{ MeV})^4}\right]$
$b_2$	$-\frac{1}{(410 \text{ MeV})^4}$	$\left[-\frac{1}{(394 \text{ MeV})^4}, -\frac{1}{(428 \text{ MeV})^4}\right]$
$g_A$	0.22	[0.18, 0.27]

Table 2: Estimated parameters (NLO).

- Fit goodness:  $\begin{cases} \chi^2_{1S_0} = 0.70 \\ \chi^2_{3S_1} = 0.12 \end{cases}$

### C. Discussion

- About  $\delta$ 's function & the cut-off: The physics that we are omitting corresponds to higher resonances  $\sigma$ ,  $\rho$ ,  $\omega$  (Ref. [8]), and because of their associated energy is in the range 500-800 MeV, the cut-off,  $\Lambda$ , should be near this range. In fact, in Ref [1], the cut-off is done such that:  $m_\pi \ll \Lambda \ll M \sim 4\pi f_\pi \sim 1100 \text{ MeV}$ , which is compatible with the previous range. But in our case we have obtained a bit lower cut-off value. That is not catastrophic but a higher cut-off would have been a better result.

- About the  $a_1$ ,  $a_2$ ,  $b_1$ ,  $b_2$  parameters: Because of the potentials that we are fitting are hadronic, the order of parameters that we have obtained in the fit should be hadronic ( $\gtrsim 400\text{MeV}$ ).

That means that,  $a_1$ ,  $a_2 \gtrsim \frac{1}{(400\text{MeV})^2}$  and  $b_1$ ,  $b_2 \gtrsim \frac{1}{(400\text{MeV})^4}$ . (In [2], this parameters are stated at  $\sim \left(\frac{M}{2\pi^2}\Lambda\right)^m \sim (300\text{MeV})^{2m}$ , with  $m = 1, 2$  at LO and NLO resp.).

We have obtained a resulting parameters  $a_1$ ,  $a_2$  lower than expected, but, in contrast,  $b_1$ ,  $b_2$  agree with what we expected.

- We have seen that the axial coupling constant,  $g_A$ , changes one order of magnitude from LO to NLO. This instability can be solved assuming that at NLO the fit will be more accurate, and hence taking the latter one as a better estimation. In fact, it has been calculated in the very recent paper [10] where  $g_A = 0.27$ . This value falls within our confidence interval when we are at NLO. To convince ourselves, we have first imposed  $g_A$  obtained at NLO to LO and next  $g_A$  obtained at LO to NLO:
  - If we fit at LO imposing  $g_A$  obtained at NLO we get an acceptable fit with these  $\chi^2$ :  
 $\chi^2_{1S0} = 3.51$ ;  $\chi^2_{3S1} = 0.33$
  - But in the reverse case, which means imposing LO  $g_A$  to NLO, the fit is catastrophic: all the parameters become 0.
- Finally, we have to remark that the goodness of the fit only improves from the LO to NLO in 1S0 channel. In 3S1 channel the goodness of the fit remains with a similar low value in both orders.

## V. ONE BOSON EXCHANGE MODELS

In this last section we will briefly treat the problem under One Boson Exchange Models and compare the result with EFT. We will use OBE potential (from [8]) which includes 4 resonances:  $\pi$ ,  $\sigma$ ,  $\omega$ ,  $\rho$ :

$$V_{1S0}^{OBE} = V_0 - \frac{1}{16\pi} \left(\frac{g_A}{f_\pi}\right)^2 m_\pi^2 \frac{e^{-m_\pi r}}{r} - \frac{g_{\sigma NN}^2 e^{-m_\sigma r}}{4\pi r} + \frac{g_{\omega NN}^2 e^{-m_\omega r}}{4\pi r} - \frac{f_{\rho NN}^2 m_\rho^2 e^{-m_\rho r}}{8\pi M^2 r} \quad (13)$$

$$V_{3S1}^{OBE} = V'_0 - \frac{1}{16\pi} \left(\frac{g_A}{f_\pi}\right)^2 m_\pi^2 \frac{e^{-m_\pi r}}{r} - \frac{g_{\sigma NN}^2 e^{-m_\sigma r}}{4\pi r} + \frac{g_{\omega NN}^2 e^{-m_\omega r}}{4\pi r} - \frac{f_{\rho NN}^2 m_\rho^2 e^{-m_\rho r}}{8\pi M^2 r} \quad (14)$$

Where  $M \approx 1300\text{ MeV}$  ( $\Xi$  mass),  $m_\pi = 146\text{ MeV}$ ,  $m_\omega \approx m_\rho \approx 780\text{ MeV}$ .

- We will use once again *Wolfram Mathematica* function *NonLinearModelFit[]*.

- The fit will be done simultaneously in both channels (1S0 and 3S1) with these shared fitting parameters:  $g_A$ ,  $g_{\sigma NN}$ ,  $g_{\omega NN}$ ,  $m_\sigma$ ,  $f_{\rho NN}$ .
- $V_0$ ,  $V'_0$  will be two other fitting parameters with the same meaning that they have in the previous fits.
- We will include for each parameter its confidence interval provided by *Wolfram Mathematica* itself.

## A. Results

During the fitting tests we have obtained  $g_{\sigma NN} \sim 10^{-16}$ , we can read that result as that ( $\sigma$ ) resonance does not contribute at all. Furthermore, we have obtained  $f_{\rho NN} \sim 10$ , but since this term has multiplying factor  $1/M^2$  we can neglect that contribution. So, the only non-vanishing terms are  $\pi$  and  $\omega$  resonances and we present their fitting outcome just below:

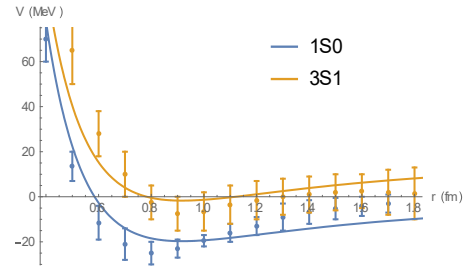


Figure 6: Fitting with OBE model of channels 1s0, 3s1.

	<i>Expected value</i>	<i>Confidence interval</i>
$g_A$	2.2	[1.5, 2.7]
$g_{\omega NN}$	21.1	[14.9, 27.3]

Table 3: Estimated parameters (OBE model).

- Fit goodness:  $\begin{cases} \chi^2_{1S0} = 2.16 \\ \chi^2_{3S1} = 0.70 \end{cases}$

## B. Discussion

It is shocking to realise that the fit removes  $\sigma$ -term: this term is not suppressed by  $\Xi$  mass (as occurs with  $\rho$ -term). Furthermore, while  $\pi$  and  $\omega$  terms are the only relevant their masses are sorted out as  $m_\pi < m_\sigma < m_\omega$ . So, it is not clear in which order should contribute each resonance. Also, adding more resonances does not seem to improve the fit: we obtain almost the same fit parameter with or without  $\rho$ ,  $\sigma$  resonances.

In contrast, in the EFT we have seen that we have a clear contribution hierarchy: We could expect that fit will improve as many terms we add and we can quantify the contribution of each order.

## VI. SCATTERING LENGTHS

In this section, we will compute numerically the scattering length of all the potentials that we have covered in

this project using the J-Matrix code provided freely in Ref. [9] which computes the phase shift. Using this code, we are able to compute the scattering length by iterating the product ( $k * \cot \delta_0(k)$ ) with decreasing  $k$ , till it converges. Where  $\delta_0(k)$  is the phase shift when the incident particle has an angular momentum  $l$ , and a wave number  $k$ , then we have,

$$\frac{1}{a_s} = - \lim_{k \rightarrow 0} k * \cot \delta_0(k).$$

In order to compute the scattering lengths, we will use the EFT potentials at LO, NLO and the OBE potentials all of them projected for channels  $1S_0$  and  $3S_1$  (discussed in section II and V resp.). As potentials parameters we will use the expected value obtained in the fit (table 1, table 2 and table 3 resp.). Also, we will estimate the error of these scattering lengths by computing them with the same potentials but changing their fitted parameters within their confidence interval, and taking the spectrum of each scattering length as its confidence interval.

In the following, we present the results at LO and NLO of EFT:

	<i>Expected value</i>	<i>Confidence interval</i>
$a_s(^1S_0)$	1.79 fm	[1.64 fm, 1.97 fm]
$a_s(^3S_1)$	3.18 fm	[2.93 fm, 3.56 fm]

Table 4: Scattering lengths at LO.

	<i>Expected value</i>	<i>Confidence interval</i>
$a_s(^1S_0)$	1.77 fm	[1.67 fm, 1.92 fm]
$a_s(^3S_1)$	2.50 fm	[2.06 fm, 3.31 fm]

Table 5: Scattering lengths at NLO.

And the results using OBE potential we have fitted:

	<i>Expected value</i>	<i>Confidence interval</i>
$a_s(^1S_0)$	1.73 fm	[1.01 fm, 2.42 fm]

$a_s(^3S_1)$	1.91 fm	[0.87 fm, 2.69 fm]
--------------	---------	--------------------

Table 6: Scattering length (OBE).

Note that the scattering lengths that we have just calculated have the typical scale we would expect within strong interaction frame.

It is also interesting to note that while  $a_s(^1S_0)$  is remarkably stable (and thus we can rely on that value),  $a_s(^3S_1)$  has a strong dependence on the fit.

## VII. CONCLUSION

- We have seen that the system  $\Xi\Xi$  behaves likewise NN, and we can describe it using the same EFT.
- Also, we have seen that EFT, unlike OBE models, provides a consistent method to construct NN potentials. Furthermore, EFT reproduce  $\Xi\Xi$ -potential more accurately than OBE models, according to our results.
- Using NLO EFT potential we have obtained a  $g_A$  estimation which agree with [10].
- We have calculated scattering lengths of  $\Xi\Xi$  in  $^1S_0$  and  $^3S_1$  channels using all the potentials covered in this project.
- To sum up, we have learnt that we are able to estimate relevant EFT parameters such as  $g_A$  by using lattice QCD results. Then, we have seen that we can make use of these EFT parameters to get physical quantities that can be measured such as scattering length.

## Acknowledgments

I would like to thank my advisor Joan Soto for all his helpful comments as well as guidance that he provided me when carrying out this project. I would also like to thank my family and friends for all their support.

- |   |  |
|---|--|
| [1] D. Eiras, J. Soto, Eur.Phys.J. A17 (2003) 89-102.   | [7] N. Ishii et al. PoS LATTICE2015 (2016) 087.  |
| [2] Silverno Pavón Valderrama, Manuel. (2018). "La interacción nucleón-nucleón en teorías efectivas" (PhD thesis). Universidad de Granada, Spain. | [8] A. Calle Cordon, E. Arriola (2010). Phys.Rev. C81:044002.  |
| [3] Rentmeester, Mart C. M., et al. Phys.Rev.Lett.82:4992-4995,1999.  | [9] P. Syty, "The J-matrix method: numerical computations", TASK Quarterly 3 No. 3 (1999).   |
| [4] J.J. Sakuray, Modern Quantum Mechanics, Redwood City: Addison-Wesley, 1985.   | [10] Aditya Savanur, Huey-Wen Lin (2018). "Lattice-QCD Determination of the Hyperon Axial Couplings in the Continuum Limit". arXiv:1901.00018. |
| [5] Machleidt, R. Int.J.Mod.Phys. E26 (2017) no.11, 1730005.  |  |
| [6] Kaiser, N, Brockmann, R, Weise, Wolfram. Nucl.Phys. A625 (1997) 758-788.  |  |